Electrical and Optical Properties of Vitreous Selenium*

H. P. D. LANYON

University of Illinois, Urbana, Illinois

(Received 30 November 1962)

The space-charge limited current-voltage characteristics of evaporated layers of vitreous selenium from 2.4 to 60 μ thick are described. It is shown that both an exponential and a Gaussian distribution of states will explain these characteristics. An analytic solution is derived for the case of the exponential distribution of states: $N(\epsilon) = N_0 e^{-\epsilon/\Delta}$, where N_0 is the density of states at the valence band edge which is taken to be the origin of energy. This solution, with $N_0 \sim 10^{20}$/cm^3 eV and $\Delta = 0.067$ eV, will account for the characteristics of all the specimens independent of thickness. The model will also account for the results of the optical absorption, electron bombardment, quenching, and positive and negative photoresponse experiments of other workers. It is not possible to obtain an analytic solution for any of these cases for a Gaussian distribution of states: $N(E) = N_0 \exp\{-(E-E_{max})^2/\Delta^2\}$. However, it is shown that the distribution in energy of these states with $E_{max} = 2.35$ eV and $\Delta = 0.25$ eV fits the experimental results as well as does the exponential distribution. A Gaussian distribution of states would be expected theoretically in a disordered material such as vitreous selenium.

1. INTRODUCTION

THE technique of space-charge limited current-voltage measurements enables one to estimate the distribution of states in the forbidden gap of wide bandgap materials containing less than 10^{14}–10^{15} carriers per cc. During the past few years, this method has been applied to many materials such as CdS, ZnS, and organic insulators. Very little work seems to have been done to tie in the results from these measurements with the results of optical absorption and photoresponse experiments which can also be performed on these materials.

In this paper, the space-charge limited current-voltage characteristics of vitreous (amorphous) selenium films from 2.4 to 60 μ thick are presented. It is shown that these may be interpreted consistently in terms of a distribution of states decreasing rapidly from the edge of the valence band both as far as the characteristics of the individual specimens and the thickness dependence of the parameters determined from these characteristics are concerned. This distribution of states appears to be characteristic of the vitreous selenium. It is shown that it allows for a consistent explanation of the optical absorption, electron bombardment, quenching and positive and negative photoresponse experiments of other workers.

2. REVIEW OF PREVIOUS WORK

Selenium lies in Group VI of the periodic table. Consequently, it has two vacant orbitals available for bonding to neighboring atoms. This takes place in two distinct ways. In monoclinic selenium closed eight-membered rings are formed which are arranged parallel to one another in the crystal. On the other hand, in the

hexagonal and vitreous forms the atoms link to form spiral chains several hundred atoms long. In the hexagonal form these line up parallel to one another along the c axis whereas in the vitreous form, which is essentially a supercooled liquid, there is no long-range order, although neighboring chains tend to line up parallel to one another. This is shown by a definite short-range order up to 10 Å from any given atom. The presence of this common structural unit in the two forms leads to many similar properties.

Although selenium has been used commercially in the manufacture of rectifiers and photocells since the turn of the century and many hundreds of papers have been written on these aspects, little systematic study of its electrical and optical properties seems to have been reported prior to 1950.

Since then, measurements of the absorption spectrum of vitreous selenium have been made by a number of workers.[1–7] As shown in Fig. 1, their results are in reasonable agreement and the behavior of the absorption coefficient in the neighborhood of the absorption edge is well defined. The interesting feature of the results is that in this region the coefficient falls exponentially with photon energy, falling in the ratio $e:1$ for a change in energy of 0.067 eV (i.e., $2.8kT$). This is much slower than for several other materials such as ZnS and AgBr,[8] which also have exponential absorption edges. In all of these materials the coefficient falls off as kT per factor e.

As shown in Fig. 2, measurements have also been made of the spectral dependence of the photoresponse.[9,10]

[1] R. S. Caldwell and H. Y. Fan, Phys. Rev. 114, 664 (1959).
[2] J. J. Dowd, Proc. Phys. Soc. (London) B69, 70 (1951).
[3] M. A. Gilleo, J. Chem. Phys. 19, 1291 (1951).
[4] H. Gobrecht and A. Tausend, Z. Physik 161, 205 (1961).
[5] W. F. Koehler, F. K. Odencrantz and W. C. White, J. Opt. Soc. Am. 49, 109 (1959).
[6] E. W. Saker, Proc. Phys. Soc. (London) B65, 785 (1952).
[7] J. Stuke, Z. Physik 134, 194 (1953).
[8] See, for example, T. S. Moss, *Optical Properties of Semiconductors* (Butterworths Scientific Publications, Ltd., London, England, 1959), p. 39.
[9] P. K. Weimer and A. D. Cope, R.C.A. Rev. 12, 314 (1951).
[10] T. S. Moss, *Photoconductivity in the Elements* (Butterworths Scientific Publications, Ltd., London, England, 1952).

If the optical absorption corresponds to band-to-band transitions, one would expect the absorption and photoresponse edges to coincide. As can be seen from the figure, which is a plot of the relative absorption and photoresponse of a 10-μ specimen as a function of the photon energy, this is not the case with vitreous selenium. The photoresponse edge lies at a higher energy than the absorption edge.

Measurements of the electron-bombardment induced and electrical properties[9,11-14] have also been reported. This work showed that vitreous selenium is a p-type material, although both electrons and holes are mobile. The hole mobility is the same as in the hexagonal form. In both materials it is characterized by an activation energy of 0.14 eV. From a consideration of the probable nature of the levels controlling the mobility the hole mobility in the valence band has been estimated to be 60 cm²/V-sec. This value has been used in the interpretation of the space-charge limited current-voltage characteristics.
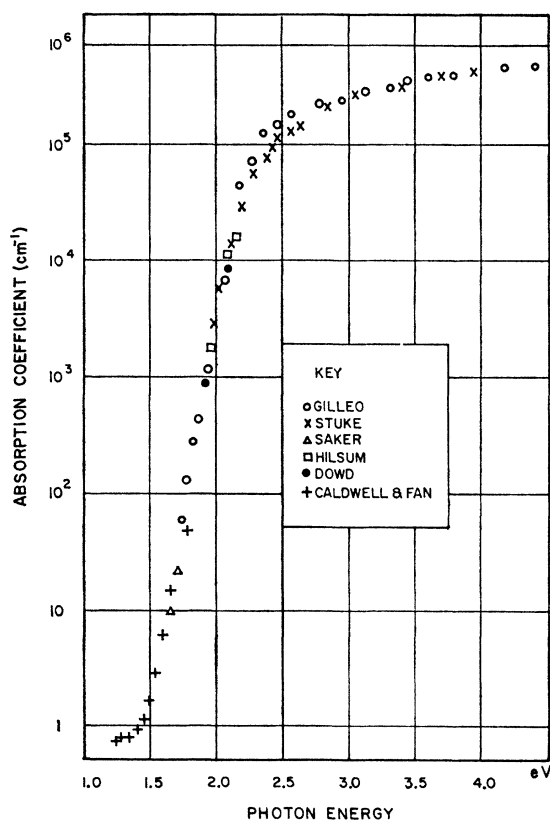

FIG. 1. Results of optical absorption experiments showing the exponential fall of the absorption coefficient with photon energy at the absorption edge.

[11] W. E. Spear, Proc. Phys. Soc. (London) **B68**, 991 (1955).
[12] W. E. Spear, Proc. Phys. Soc. (London) **B70**, 669 (1957).
[13] W. E. Spear and H. P. D. Lanyon, in *Proceedings of the International Conference on Semiconductor Physics, Prague, 1960* (Czechosolovakian Academy of Sciences, Prague, 1961), p. 987.
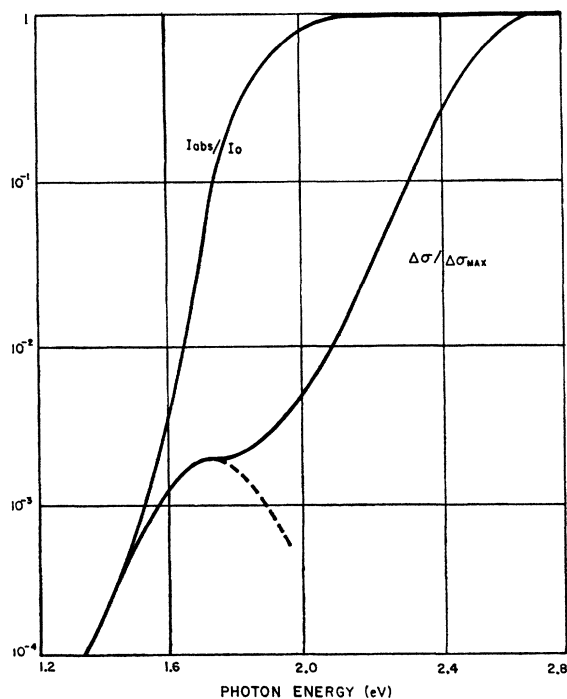[14] W. E. Spear, Proc. Phys. Soc. (London) **76**, 826 (1960).

FIG. 2. Comparison of the optical absorption and photoresponse edges. The photoresponse edge ($\Delta\sigma/\Delta\sigma_{max}$) lies at higher photon energies and is not related in a simple manner to the power absorbed, (I_{abs}/I_0).

3. SPACE-CHARGE LIMITED CURRENTS

The main features of the current-voltage characteristics have already been described elsewhere.[13,15] The measurements were made on evaporated layers of vitreous selenium sandwiched between platinum or tellurium electrodes. Care was taken to avoid contamination of the interface by maintaining a high vacuum throughout the preparation of the specimens. Measurements of the characteristics were made quasi-statically, allowing time for the current to reach a steady value except where it is stated to the contrary. The measurements were made with increasing voltage.

As shown in Fig. 3, the specimens often did not show an Ohmic region at low voltages on first applying a field. It was only after the application of a large field for some time that the specimen became "formed." Several stages in the forming of a specimen are shown. It is seen that the maximum field applied during the first run was not sufficient to form the specimen. On the other hand, after the second run the specimen shows an Ohmic region at low voltage and the current has increased by many orders of magnitude in this region. The conductivity has increased even further in the fourth run. The reduction in current at high fields on forming is probably not a genuine effect. In order to avoid too much forming, it is necessary to make the

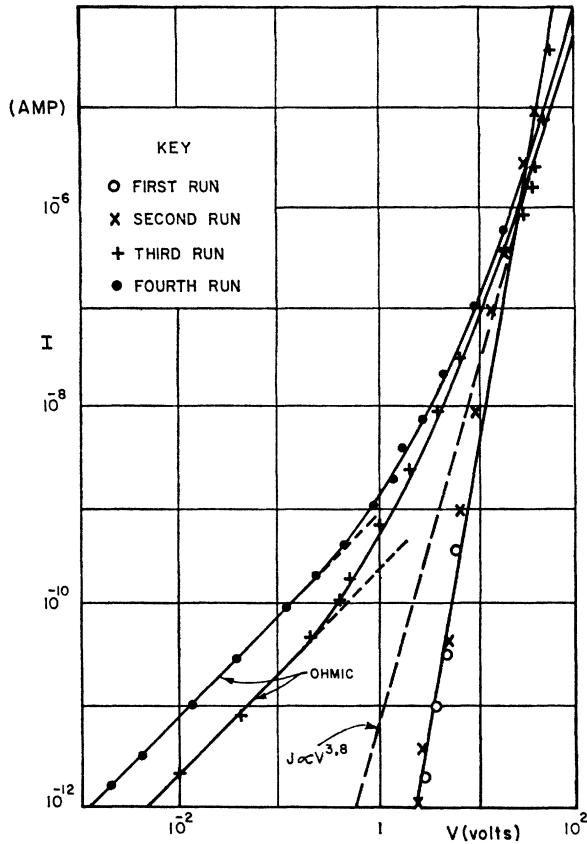[15] H. P. D. Lanyon and W. E. Spear, Proc. Phys. Soc. (London) **76**, 1157 (1961).

FIG. 3. Stages in the "forming" of a 28-μ thick specimen carrying tellurium electrodes.

early measurements quickly before the specimen current has become completely steady (and hence come to equilibrium). The third and fourth characteristics are typical of those of formed specimens. They have an Ohmic region at low voltages showing that the contact is "Ohmic." At higher voltages, the current increases less quickly with voltage than for a discrete level, showing that the Fermi level is being moved through a distribution of states by the voltage injection of additional carriers. In the high-voltage region, the characteristics of many specimens followed the relationship: $J \propto V^{3.8}$. Rose[16] has shown that such a power-law dependence of space-charge limited currents occurs with an exponential distribution of states.

It is possible to obtain an analytic solution for this case provided that the diffusive component to the current is neglected. It is not possible to obtain an analytic solution for the case of a Gaussian distribution of states in energy. However, it is shown in the discussion (Sec. 5) that close to the center of the bandgap, the distribution in energy of the states is very similar to that for the exponential distribution. Consequently, the results obtained for the exponential distribution will not be substantially different from those for the

16 A. Rose, Phys. Rev. **97**, 1538 (1955).

Gaussian distribution which would be expected theoretically in a disordered material such as vitreous selenium.

As shown in Fig. 4, the exponential distribution of states to be considered is

$$N(\epsilon) = N_0 e^{-\epsilon/\Delta}, \tag{1}$$

where N_0 is the density of states at the valence band edge and Δ characterizes the rate at which the states fall off with energy. In the absence of voltage there are $\bar{P}_{tot}$ holes present and the Fermi level lies ζ_p above the valence band. A quick derivation of the current- voltage characteristic can be made provided that a uniform distribution of charge and electric field are assumed throughout the specimen.

When a voltage V is applied, an additional density of holes proportional to the applied voltage will be injected into the specimen, moving the Fermi level to a new position, ζ_s. Let us call this injected density, αV. A calculation of α will be given later in the Appendix. Provided that $\Delta \gg kT$ it can be assumed that all of this charge will condense into the traps so that the total of trapped holes, p_t, is given by

$$p_t = \bar{p}_t + \alpha V, \tag{2}$$

where $\bar{p}_t$ is the density of trapped holes in the absence of voltage. Let us define a quantity, V_A, by

$$\bar{p}_t = \alpha V_A. \tag{3}$$

Then we have

$$p_t = \alpha(V + V_A). \tag{4}$$

Now p_t is equal to the density of states above the Fermi level in the case we are considering so that

$$p_t = \Delta N_0 e^{-\zeta_s/\Delta}. \tag{5}$$

Also, we have for the density of free carriers in the valence band:

$$p = N_v e^{-\zeta_s/kT}, \tag{6}$$

where N_v is the effective density of states in the valence band. This gives us that

$$p \propto p_t^{\Delta/kT} \tag{7}$$

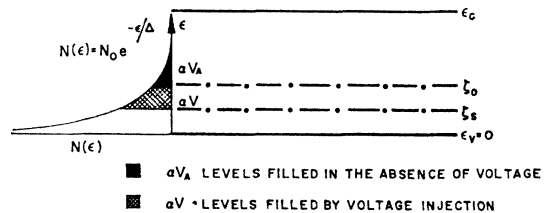independently of the position of the Fermi level. This is a most important relationship which will be used

FIG. 4. Proposed exponential distribution of states in vitreous selenium. The movement of the Fermi level from ζ_0 to ζ_s by the voltage injection of additional holes is shown.
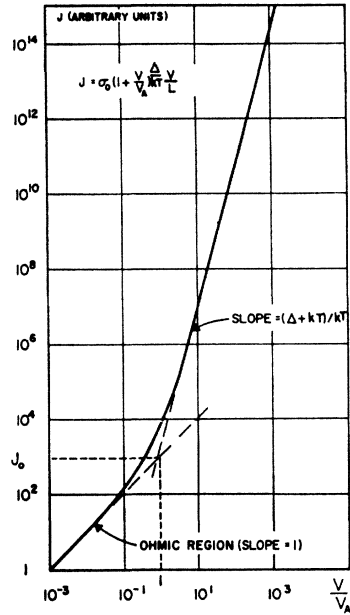
FIG. 5. Theoretical $J-V$ characteristic for an insulator with an exponential distribution of states. At low voltages Ohm's law holds; at high voltages: $J \propto V^{(\Delta+kT/kT)}$.

several times. From it we now have that

$$p \propto (V+V_A)^{\Delta/kT} \qquad (7a)$$

and

$$\bar{p} \propto V_A{}^{\Delta/kT} \qquad (7b)$$

so that

$$\sigma/\sigma_0 = pe\mu/\bar{p}e\mu = (1+V/V_A)^{\Delta/kT} \qquad (8)$$

and

$$J = \sigma_0(1+V/V_A)^{\Delta/kT}(V/L), \qquad (9)$$

where L is the specimen thickness. This is shown on a logarithmic plot in Fig. 5.

At low voltages, there is negligible injection of holes and we have an ohmic region characterized by the conductivity, σ_0. Knowing σ_0 and the mobility of free holes from Spear's drift mobility measurements we can estimate the density of holes in the valence band in the absence of voltage and hence the position of the Fermi level. This last value is independent of the effective mass of holes used to estimate the effective density of states in the valence band since this cancels out. However, the recent measurements of the Faraday rotation[17] of polarized light in vitreous selenium well away from the absorption edge will lead to a revised estimate for the mobility of holes in the valence band: $\mu_0 = 10$ cm^2/V-sec.

At high voltages, the density of holes present in thermal equilibrium is negligible compared with that injected and we obtain Rose's relationship: $J \propto V^{(\Delta+kT)/kT}$. This is a straight line of slope $(\Delta+kT)/kT$ on the logarithmic plot. This slope gives the most convenient method of determining Δ. Once this has been done the shape of the curve is completely defined. For vitreous

[17] H. Gobrecht, A. Tausend, and I. Bach, Z. Physik 166, 76 (1962).

selenium specimens the slope in the high voltage limit is 3.8 which gives $\Delta = 2.8kT$ $(= 0.067$ eV).

From the fit of the theoretical curve to experimental characteristics two quantities may be determined, corresponding to the normalizing constants for the current and voltage axes—in other words these determine the position of the origin of coordinates. These have been taken to be V_A, the voltage at which the total density of free holes (free plus trapped) has been doubled by voltage injection, and J_0, the current which would flow at V_A in the absence of injection. These quantities have been determined from fits of the theoretical curve with $T_c = 2.8T$ to the experimental characteristics of 28 runs on 15 specimens from 2.4 to 60 μ thick. The results are given in Table I. A typical fit is shown in Fig. 6. The only other measurements of space-charge limited current-voltage characteristics in vitreous selenium have been made by Hartke[18] who also repeated Spear's measurement of the drift mobility of carriers. It is of interest that all three of his experimental characteristics may be fitted to the same theoretical curve with $\Delta = 0.067$ eV as is shown in Fig. 7. Since the selenium came from different sources this is strong evidence that the distribution of states is characteristic of the vitreous selenium and is not

TABLE I. Parameters obtained from the fit of the theoretical current-voltage characteristic to the experimental points for a number of specimens of different thicknesses. Runs on the same specimen are bracketed.

$L(\mu)$	V_A (V)	J_0 (A/cm^2)	σ_0 (Ω cm)$^{-1}$	V_A/L^2 (V/cm^2)	$J_0(L/10)^{6.6}$
2.4	1.2	5.6×10^{-10}	1.1×10^{-13}	2.1×10^7	1.1×10^{-10}
6.5	$\begin{cases} 1.2 \\ 0.9 \\ 0.8 \\ 1.1 \end{cases}$	$\begin{array}{l} 5.6 \times 10^{-10} \\ 4.4 \times 10^{-9} \\ 9.6 \times 10^{-10} \\ 1.4 \times 10^{-10} \end{array}$	$\begin{array}{l} 3.0 \times 10^{-13} \\ 3.2 \times 10^{-12} \\ 7.8 \times 10^{-13} \\ 6.4 \times 10^{-14} \end{array}$	$\begin{array}{l} 2.8 \times 10^6 \\ 2.1 \times 10^6 \\ 1.9 \times 10^6 \\ 2.6 \times 10^6 \end{array}$	$\begin{array}{l} 3.2 \times 10^{-11} \\ 2.5 \times 10^{-10} \\ 5.5 \times 10^{-11} \\ 8 \times 10^{-12} \end{array}$
8.5	$\begin{array}{l} 5.2 \\ 50 \\ 8 \end{array}$	$\begin{array}{l} 6.5 \times 10^{-9} \\ 5.5 \times 10^{-5} \\ 6 \times 10^{-7} \end{array}$	$\begin{array}{l} 1.05 \times 10^{-12} \\ 9.3 \times 10^{-10} \\ 6.4 \times 10^{-11} \end{array}$	$\begin{array}{l} 7.2 \times 10^6 \\ 6.9 \times 10^7 \\ 1.1 \times 10^7 \end{array}$	$\begin{array}{l} 2.2 \times 10^{-9} \\ 1.9 \times 10^{-5} \\ 3.2 \times 10^{-7} \end{array}$
8.6	$\begin{array}{l} 5.5 \\ 36 \end{array}$	$\begin{array}{l} 2.4 \times 10^{-7} \\ 2.7 \times 10^{-5} \end{array}$	$\begin{array}{l} 3.8 \times 10^{-11} \\ 6.5 \times 10^{-10} \end{array}$	$\begin{array}{l} 7.4 \times 10^6 \\ 4.9 \times 10^7 \end{array}$	$\begin{array}{l} 9.6 \times 10^{-8} \\ 1.1 \times 10^{-5} \end{array}$
9	26	4.4×10^{-5}	1.5×10^{-9}	3.2×10^7	2.3×10^{-5}
	$\begin{cases} 4^a \\ 3.8^b \\ 3.4 \end{cases}$	$\begin{array}{l} 5.5 \times 10^{-8} \\ 3 \times 10^{-8} \\ 1.8 \times 10^{-8} \end{array}$	$\begin{array}{l} 1.25 \times 10^{-11} \\ 7.1 \times 10^{-12} \\ 4.8 \times 10^{-12} \end{array}$	$\begin{array}{l} 4.9 \times 10^6 \\ 4.7 \times 10^6 \\ 4.2 \times 10^6 \end{array}$	$\begin{array}{l} 2.9 \times 10^{-8} \\ 1.9 \times 10^{-9} \\ 9.6 \times 10^{-9} \end{array}$
12	$\begin{cases} 4.5 \\ 4 \\ 2.8 \end{cases}$	$\begin{array}{l} 3.6 \times 10^{-8} \\ 1.8 \times 10^{-8} \\ 3 \times 10^{-10} \end{array}$	$\begin{array}{l} 9.6 \times 10^{-12} \\ 5.4 \times 10^{-12} \\ 1.3 \times 10^{-13} \end{array}$	$\begin{array}{l} 3.1 \times 10^6 \\ 2.8 \times 10^6 \\ 1.9 \times 10^6 \end{array}$	$\begin{array}{l} 1.2 \times 10^{-7} \\ 6.1 \times 10^{-8} \\ 1.0 \times 10^{-9} \end{array}$
14	$\begin{cases} 16 \\ 20 \end{cases}$	$\begin{array}{l} 4.6 \times 10^{-9} \\ 1.5 \times 10^{-9} \end{array}$	$\begin{array}{l} 4.0 \times 10^{-13} \\ 1.05 \times 10^{-13} \end{array}$	$\begin{array}{l} 8.2 \times 10^6 \\ 1.0 \times 10^7 \end{array}$	$\begin{array}{l} 4.2 \times 10^{-8} \\ 1.4 \times 10^{-8} \end{array}$
14.6	140	1.5×10^{-5}	1.55×10^{-10}	6.6×10^7	1.8×10^{-4}
21	$\begin{array}{l} 6.2^c \\ 31^c \\ 45^c \end{array}$	$\begin{array}{l} 3.1 \times 10^{-13} \\ 4 \times 10^{-10} \\ 1.4 \times 10^{-10} \end{array}$	$\begin{array}{l} 1.05 \times 10^{-15} \\ 2.7 \times 10^{-14} \\ 6.5 \times 10^{-15} \end{array}$	$\begin{array}{l} 1.4 \times 10^6 \\ 7.0 \times 10^6 \\ 1.0 \times 10^7 \end{array}$	$\begin{array}{l} 4.1 \times 10^{-11} \\ 5.2 \times 10^{-8} \\ 1.8 \times 10^{-8} \end{array}$
28	$\begin{array}{l} 0.48 \\ 2.5 \end{array}$	$\begin{array}{l} 1 \times 10^{-13} \\ 6.3 \times 10^{-10} \end{array}$	$\begin{array}{l} 6 \times 10^{-13} \\ 7.2 \times 10^{-10} \end{array}$	$\begin{array}{l} 6.1 \times 10^5 \\ 3.2 \times 10^6 \end{array}$	$\begin{array}{l} 5.4 \times 10^{-9} \\ 6.5 \times 10^{-7} \end{array}$
31	44	2.9×10^{-9}	2.0×10^{-13}	4.6×10^6	5.2×10^{-6}
	$\begin{cases} 15 \\ 16 \end{cases}$	$\begin{array}{l} 7.4 \times 10^{-11} \\ 6 \times 10^{-11} \end{array}$	$\begin{array}{l} 1.5 \times 10^{-14} \\ 1.15 \times 10^{-14} \end{array}$	$\begin{array}{l} 1.6 \times 10^6 \\ 1.7 \times 10^6 \end{array}$	$\begin{array}{l} 1.3 \times 10^{-7} \\ 1.1 \times 10^{-7} \end{array}$
60	50	1×10^{-12}	1.2×10^{-16}	1.4×10^6	1.3×10^{-7}

a 4 runs.
b 2 runs.
c Hartke.

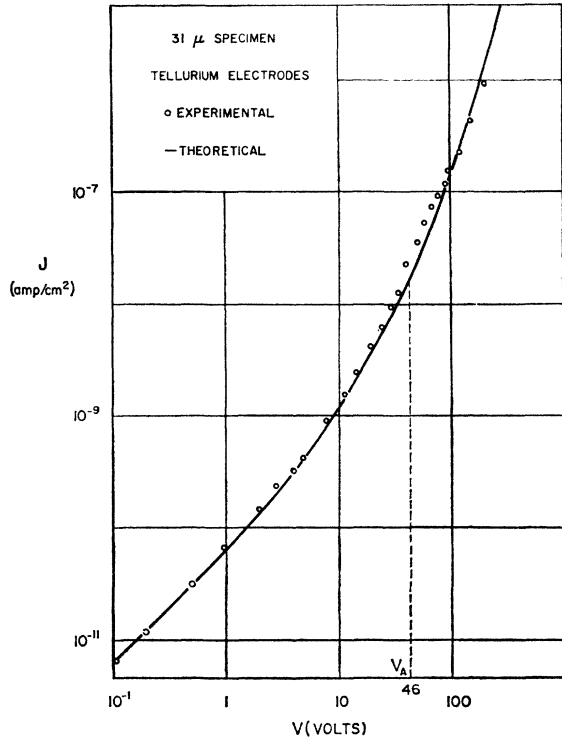[18] J. L. Hartke, Phys. Rev. 125, 1177 (1962).

Fig. 6. Typical fit of the theoretical law of Fig. 5 to the experimental results for a vitreous selenium specimen 31μ thick. Δ has been taken as $2.8kT$.

produced by an impurity present in any one sample of selenium.

An interesting check on this can be made from the thickness dependence of V_A and J_0. It was shown earlier [Eq. (7)] that the density of free holes was related to that trapped by the relationship: $p \propto p_t{}^{\Delta/kT}$. This holds independently of the position of
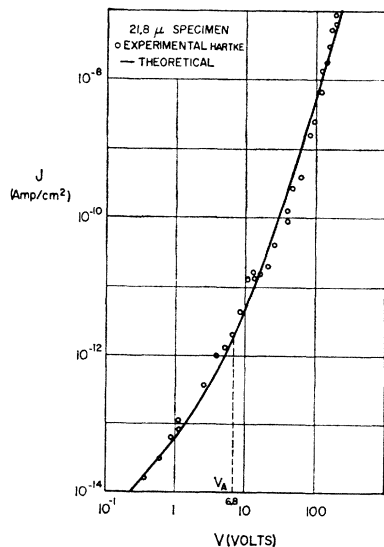
Fig. 7. Fit of the theoretical law with $\Delta = 2.8kT$ to Hartke's experimental results for a specimen 21.8μ thick.

the Fermi level provided that the distribution of traps remains unaltered. This enables us to derive a relationship between J_0, V_A, and L provided that the traps are distributed uniformly throughout the bulk of the specimen and are not states produced at the surface during the forming process.

In this case, from the definition of V_A and J_0 we have from Equation (3)

$$\bar{p}_t = \alpha V_A$$

and

$$J_0 = \bar{p}e\mu V_A/L. \tag{10}$$

Since

$$\bar{p} \propto \bar{p}_t{}^{\Delta/kT} \propto (V_A)^{\Delta/kT},$$

this reduces to

$$J_0 \propto (\alpha V_A)^{\Delta/kT} V_A/L. \tag{11}$$

Rose[19] has shown from a simple consideration of the charge on the plates of a capacitor that the constant α should be given approximately by:

$$\alpha = \epsilon/4\pi L^2 e.$$

It is shown in the Appendix [Eq. (A9)] that the same answer, but with the additional constant of proportionality $(2\Delta + kT)/(\Delta + kT)$, follows from a detailed consideration of the charge distribution in the presence of an exponential distribution of traps.

If this thickness dependence of α is fed into the relationship between J_0 and V_A, we get

$$J_0 \propto (V_A/L^2)^{\Delta/kT} V_A/L, \tag{12}$$

and finally

$$J_0 L^{(2\Delta + kT)/kT} \propto V_A{}^{(\Delta + kT)/kT}. \tag{13}$$

For vitreous selenium, with $\Delta = 2.8kT$, this should become

$$J_0 L^{6.6} \propto V_A{}^{3.8}$$

if we have an exponential distribution of states in the volume which is characteristic of the selenium itself.

In Fig. 8 a plot of $J_0 L^{6.6}$ against V_A has been made on a logarithmic scale using all of the experimental points available. This should be a straight line of slope 3.8. The fit to the best straight line of this slope, which has been drawn through the points, is as good as could be expected. The main sources of error arise from the thickness determination (any error being magnified by the high power to which it is raised) and from the arbitrariness of the fit of the experimental points to the theoretical curve. It will be seen that there is a systematic error between Hartke's results and those obtained at Leicester, although each defines a straight line of slope 3.8. This is most likely due to an error in thickness determination.

An alternative way of representing these results is to plot the Ohmic conductivity, σ_0 (which is proportional to the density of free carriers) against the density of trapped carriers present in the absence of voltage (proportional to V_A/L^2). This is not as satisfactory as

[19] A. Rose, R. C. A. Review 12, 362 (1955).

the previous plot as the thickness is used in the determination of both σ_0 and V_A/L^2. However, the plot in Fig. 9 does show directly the position of the Fermi level. In this plot the agreement with the theoretical line (of slope 2.8) is not as good as in Fig. 8. However, there is a definite correlation between the experimental points and this line. From the plot it can be seen that the Fermi level lies in the range from 0.6 to 1.1 eV above the valence band. This value is most certainly not a constant of the material. Presumably the variation is due to the presence of impurities. It is possible that this is caused by the diffusion of tellurium from the electrode into the bulk. Recent measurements by Boltaks and Plachenov[20] on the self-diffusion of selenium
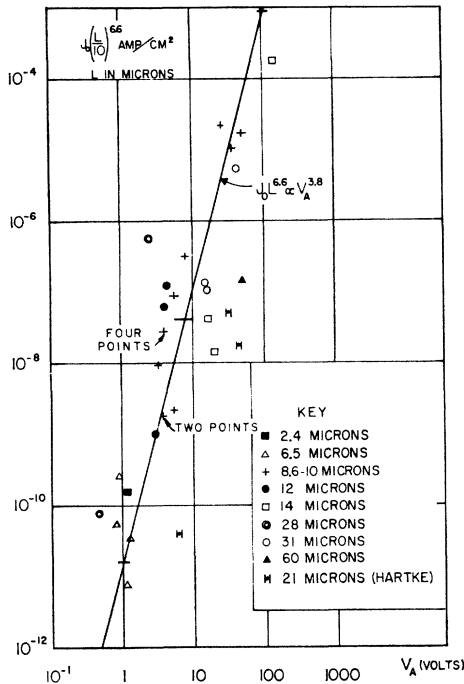
FIG. 8. Comparison of the experimental results of 28 runs on 15 specimens from 2.4 to 60μ thick with the theoretical relationship: $J_0 L^{6.6} \propto V_A^{3.8}$, which should hold for the exponential distribution of states in vitreous selenium.

suggest that there could be significant diffusion of tellurium, particularly when it is field-driven by the high fields applied during the forming process. The fact that forming continues after an Ohmic region is observed is strong evidence in favor of this as one mechanism of forming. Also, it has never been found possible to observe the forming of only one contact as would be expected if the forming were purely a surface effect.

From the results shown on the last two figures it is possible to estimate that N_0, the density of states at the valence band edge, is of the order of $10^{20}/\text{eV-cm}^3$. It must be emphasized that the space-charge limited

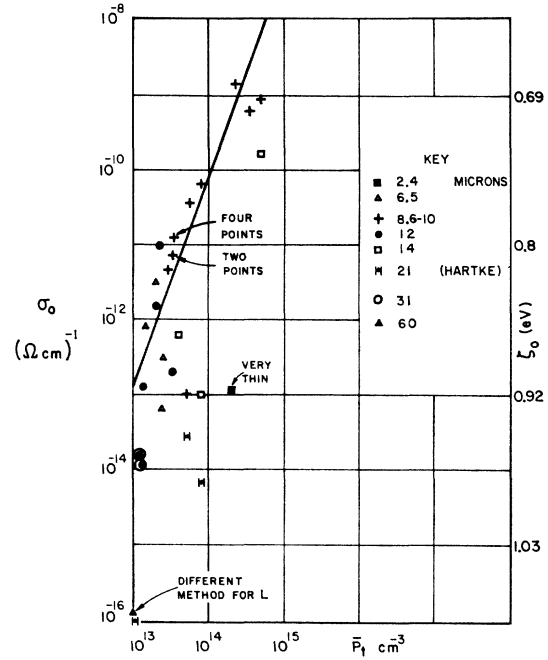[20] B. I. Boltaks and B. Plachenov, Soviet Phys.—Tech. Phys. 2, 2071 (1957).

FIG. 9. Plot of the Ohmic conductivity, σ_0, against the total density of carriers in the absence of injection, $\bar{P}_t$, showing the variation in Fermi level from specimen to specimen.

current-voltage characteristics can only give information about the distribution of states in the limited energy region through which the Fermi level passes. This is restricted by the breakdown strength of selenium ($\sim 2 \times 10^5$ V/cm). However, it is possible to obtain evidence of the states in the neighborhood of the band edge from a consideration of the absorption coefficient in the region of the absorption edge.

4. OPTICAL EXPERIMENTS

1. Optical Absorption

As shown in Fig. 10, absorption of light takes place by the excitation of an electron from a filled state to an
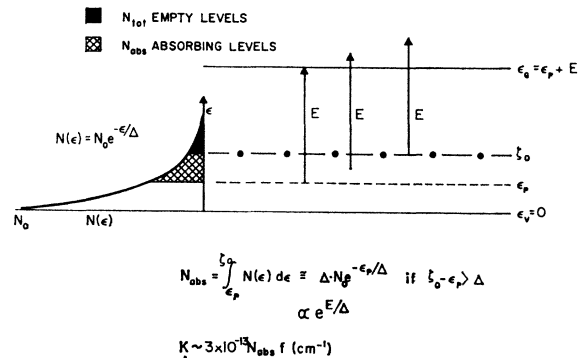

FIG. 10. Absorption scheme for vitreous selenium. The shaded levels above the Fermi level, being empty of electrons, cannot contribute to the absorption. Only those filled levels (cross-hatched) closer to the conduction band than the photon energy, E, contribute to the absorption.
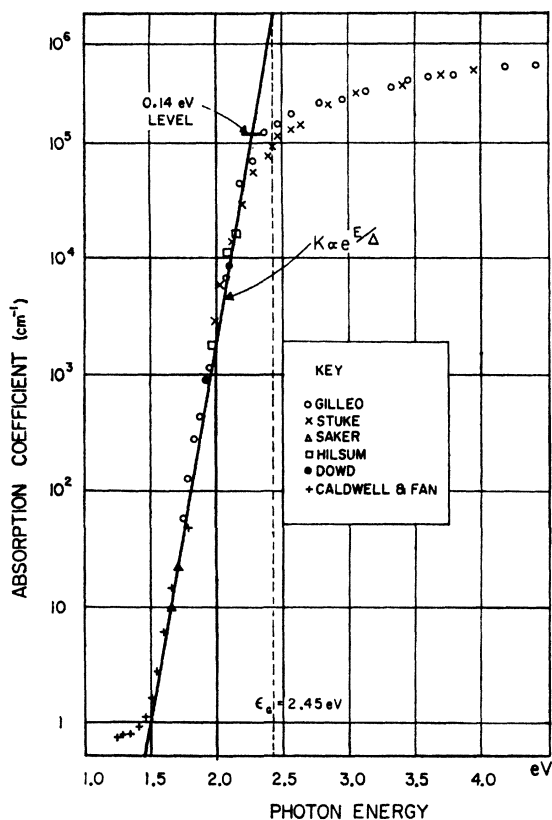
FIG. 11. Comparison of the theoretical absorption edge for an exponential distribution of states in vitreous selenium with the experimental results shown in Fig. 1. In this interpretation the bandgap, $\epsilon_G = 2.45$ eV.

empty one; for example, from the valence band to the conduction band. In the case of vitreous selenium there will also be absorption due to the exponential distribution of states in the forbidden gap. The demarcation line between the empty and the filled states in this distribution is the Fermi level, ζ_0. Absorption will take place by excitation from the filled states below the Fermi level to the conduction band. Excitation from the valence band into the empty states and from full states into the empty states in the distribution is negligible in the range of photon energies considered.

The absorption coefficient[21] of a medium is given by

$$K = (\pi e^2/nm)N_{abs}f, \tag{14}$$

where e and m are the electronic charge and mass, n is the refractive index of the medium, and N_{abs} is the density of states contributing to the absorption. f is the oscillator strength, which is of the order of unity for an allowed transition. In the case of vitreous selenium, if a typical value of 2.5 is used for the refractive index, this becomes

$$K \propto 3 \times 10^{-13} N_{abs} \text{ cm}^{-1}.$$

_____

[21] See, for example, H. Y. Fan, in *Reports on Progress in Physics* (The Physical Society, London, 1956), Vol. 19, p. 107.

If photons of energy E are absorbed, all those filled states which are closer to the conduction band than E will contribute to the absorption as shown in the figure. If the photon energy corresponds to excitation from an energy ϵ_p in the exponential distribution (which is measured from the valence band edge so that $\epsilon_p + E = \epsilon_G$, the gap width) all those states between the Fermi level and ϵ_p will contribute to the absorption. These states have been cross-hatched in the figure. Provided that $\zeta_0 - \epsilon_p \gg \Delta$, one may neglect the empty states above the Fermi level (shaded in the figure) and the density (in space) of absorbing states is given by

$$N_{abs} = \int_{\epsilon_p}^{\zeta_0} N_0 e^{-\epsilon/\Delta} d\epsilon \cong \Delta N_0 e^{-\epsilon_p/\Delta} \tag{15}$$

so that

$$N_{abs} \propto e^{E/\Delta}. \tag{15a}$$

The theoretical absorption edge is therefore exponential, the coefficient falling in the ratio $e:1$ for a change in photon energy of Δ. This agrees well with the experimental edge, as is shown in Fig. 11. Since the trap distribution has been determined completely from the current-voltage characteristics, it should be possible to calculate the absorption curve without the use of any *ad hoc* parameters if the gap width were known (provided that f were taken to be unity). Alternatively the gap width may be estimated from a numerical fit to the absorption curve. Thus, for a photon energy corresponding to excitation from the valence band to the conduction band all the states in the exponential distribution will contribute to the absorption (i.e., $\Delta N_0 = 6.7 \times 10^{18}/\text{cm}^3$) leading to an absorption coefficient, $K = 2 \times 10^6$ cm^{-1}. It can be seen from the figure that if the exponential edge were to continue to higher photon energies this absorption would occur at $E = 2.45$ eV which corresponds to the gap width. It is interesting that the break from the exponential edge occurs at 2.3 eV which would correspond to the activation energy of 0.14 eV for the hole mobility found by Spear and Hartke. The optical data confirm that in the region of the Fermi level (which corresponds to photons of energy 1.5–1.9 eV) there is still an exponential distribution of states.

2. Photoconductivity

It is difficult to make any quantitative comparison of the experimental photoresponse curves with the theoretical dependence of an exponential distribution of states, as there are many unspecified variables.

In the simplest possible model, electrons are excited from states in the exponential distribution into the conduction band. The electrons will contribute to the current at all photon energies whereas the holes will only contribute when they are left in states which are sufficiently close to the valence band for significant thermal excitation to occur into it. Qualitatively, this

will account for the difference in energy of the optical absorption and photoconductive edges. The optical absorption at long wavelengths occurs by excitation from the discrete states, only giving rise to an electron current. There is a marked increase in the current at a photon energy of 2.3 eV which would correspond to excitation from the 0.14-eV levels associated with the hole mobility. The details of the response curve depend in a complicated way on the ratio of the depth of penetration of the light to the range of the carriers (which in turn will depend on the applied electric field and, for a bimolecular recombination mechanism, on the intensity of illumination) and to the specimen thickness. In addition, it is probable that many of these quantities will have different values in the surface region where much of the excitation occurs. More careful experimental work needs to be done before any check on this interpretation can be made.

It is interesting that Dresner[22] has observed both negative photoconductivity and long-wavelength quenching of photoconductivity in vitreous selenium layers. Both showed a maximum for light of energy between 1.9 and 2.1 eV. These effects may both be associated with the excitation of a (low mobility) minority carrier which recombines with the majority carrier. In the case of vitreous selenium, electrons are excited from the exponential trap distribution leaving trapped holes which do not take part in the conduction. If the recombination cross section with free holes is sufficiently large, the electrons will recombine with the holes already present, so reducing the current flowing through the specimen. If there is no other illumination, this results in a negative photoconductivity; with illumination, quenching is produced. It is interesting that Dresner observed the maximum of both these effects in just the spectral range in which most states in the exponential distribution are available to contribute to the negative effects.

3. Photo- and Electron-Bombardment-Induced Conductivity

Some unpublished results[23] on the intensity dependence of the photoconductivity and electron-bombardment-induced conductivity are of interest. Using high-energy electrons which completely penetrated the selenium, Spear studied the secondary current as a function of the bombarding current. Figure 12(a) is a plot of the generated current (total current less the current in absence of bombardment) against the bombarding current on a log-log scale. Measurements have been made with three different fields across the specimen. Figure 12(b) shows the intensity dependence of the photocurrent in the same specimen. The light source was a tungsten lamp which had been calibrated against a selenium barrier layer cell (which was assumed

[22] J. Dresner, J. Chem. Phys. **35**, 1626 (1961).
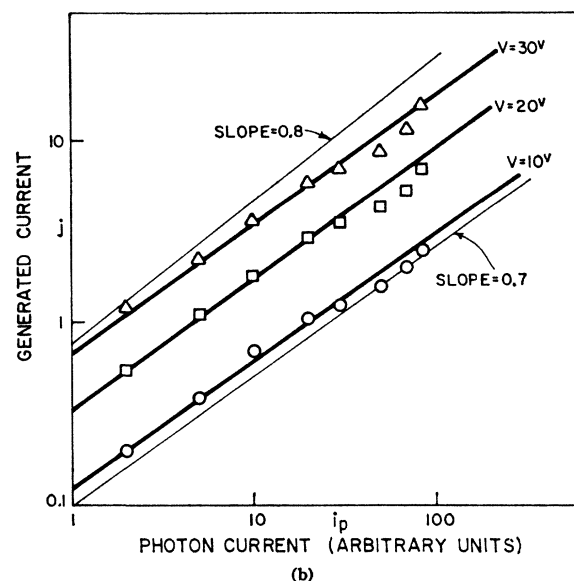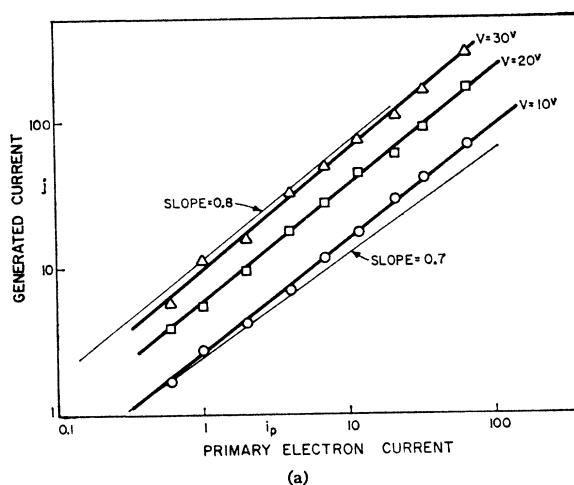[23] W. E. Spear (private communication).

Fig. 12. Gain under steady excitation. (a) Generated current (total current less the current in the absence of bombardment) produced by bombardment with electrons which completely penetrate the specimen. (b) Generated photocurrent for the same specimen (W. E. Spear, private communication). Theory gives $j \propto i_p^{0.74}$ for both of these cases.

to be linear). In both cases the secondary current is related to the primary current by the law: $j \propto i_p^n$, where n lies between 0.7 and 0.8. Rose[16] has considered the photoresponse of an insulator with an exponential distribution of states and has shown that one should get for this case: $j \propto i_p^{\Delta/(\Delta+kT)}$. For vitreous selenium, with $\Delta = 2.8kT$, this becomes $j \propto i_p^{0.74}$, which is in very good agreement with Spear's results.

5. DISCUSSION

From an analysis of the current-voltage characteristics of vitreous selenium, one can estimate the distribution in energy of states in the band gap. From the voltage at which the characteristic first departs from

Ohm's law, it is possible to estimate the position of the Fermi level and the density of states in this energy range. Thus, the characteristics were first interpreted in terms of Lampert's simplified theory for a discrete level, although it was pointed out that the slope of the characteristic was too shallow to be consistent with this model.

Hartke has taken the next step of analyzing the characteristic of terms of a uniform distribution of states in the gap. Such a distribution might arise in selenium from the broadening of an impurity level due to the variation of environment in the unordered material. On the basis of this model he was able to account for current-voltage characteristics of his specimens which were all of the same thickness. Since the Fermi level can only be moved a few kT through the band gap by the voltage injection of excess carriers, it is only possible to say that this interpretation gives the average density of states in this region. The model gives no explanation of the optical and photoelectrical properties of selenium.

If the states which have been observed here are characteristic of the vitreous selenium itself, one would expect them to be produced as a result of the varying local potential at different atomic sites. This would cause the bands to be 'smeared out' and might be expected to produce a distribution of states falling off from the band edge.

The simplest model that can take this into account and is also easily treated mathematically is that of a distribution falling off exponentially in energy. In the region of the Fermi level the density of states will not alter much in a few kT and so the current-voltage characteristic will be very similar to that found by Hartke for the uniform distribution of states. However, there will be profound differences between the two models when the measurements extend over a larger energy range. Thus the exponential model gives a reasonable account of the current-voltage characteristics of specimens with the Fermi level from 0.69 to 1.0 eV above the valence band and accounts for the exponential edge to the optical absorption curve. It also explains many of the photoelectric effects which have been observed.

Great care must be taken that too much physical significance is not attached to the exponential nature of the distribution. Other distributions can also lead to the same density of states in the energy range considered. Theoretically, one might expect that the variation in next-nearest neighbor distance in selenium would produce a Gaussian distribution of states:

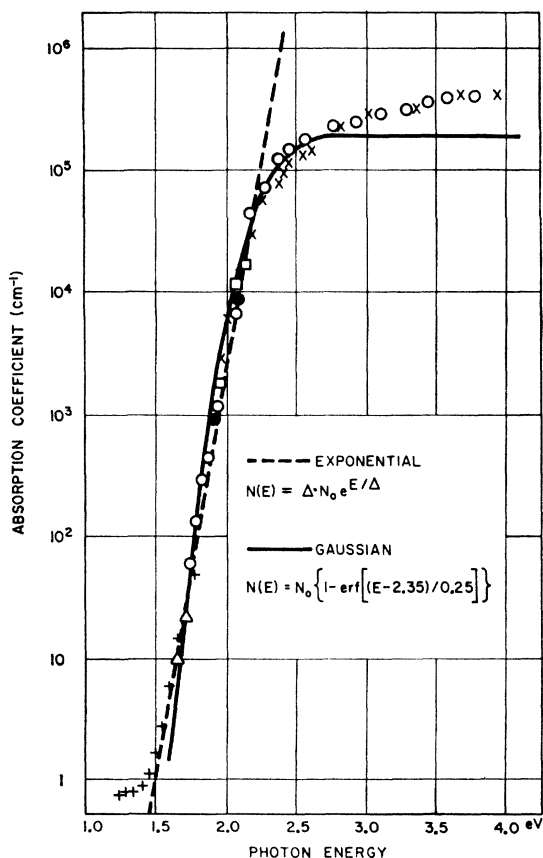$$N(E) = N_0 \exp[-(E-E_{max})^2/\Delta^2],$$

Fig. 13. Comparison of the optical absorption edges assuming an exponential and a Gaussian distribution of states. The distributions give equally good agreement with experiment up to a photon energy of 2.2 eV. The improved fit with the Gaussian distribution at higher photon energies reflects the falling density of states on the high-energy side of E_{max}.
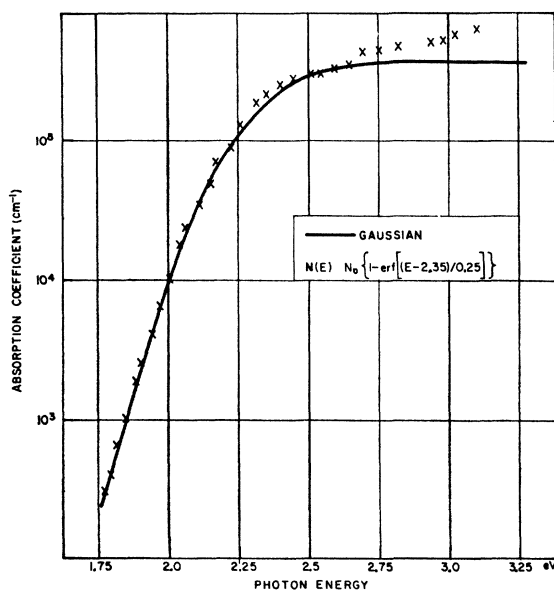

Fig. 14. Comparison of the optical absorption edge of hexagonal selenium for light with the E vector parallel to the c axis with that due to a Gaussian distribution of states in energy. The parameters are identical to those used to fit the experimental results for vitreous selenium.

with the density of states falling off on either side of the peak density at E_{max}. In Fig. 13, the density of states contributing to optical absorption has been plotted as a function of photon energy for this model using the values $E_{max}=2.35$ eV and $\Delta=0.25$ eV. This density of states is $N_0\{1-\text{erf}[(E-E_{max})/\Delta]\}$. It can be seen that this model fits the absorption edge as well as the exponential edge over the energy range in which both may be applied and also leads naturally to the break from the edge. Since the total density of states is the same for the two models as a function of energy this model would lead to essentially the same current-voltage characteristics although this has not been calculated specifically. It is interesting that this same distribution of states also accounts for the optical absorption of hexagonal selenium with the E-vector parallel to the c-axis. This has been plotted in Fig. 14, using the same values of E_{max} and Δ.

Work is now in progress to move the Fermi level further through the bandgap by doping with various elements. It is hoped that the combination of electrical and optical experiments will enable a more complete account to be made of the distribution of states in the bandgap.

Note added in proof. Recent measurements[24] of the relative quantum efficiency of photoexcitation in vitreous selenium have confirmed the model suggested here to explain the spectral distribution of the photoresponse. Using a short monochromatic light pulse, it was shown that at low-photon energies the response due to holes diminishes with respect to that of electrons, since at energies of less than 2.3 eV the holes are left in trapping levels from which they must be thermally excited before they can contribute to the electrical current.

ACKNOWLEDGMENTS

[24] J. L. Hartke and P. J. Regensburger, Bull. Am. Phys. Soc. 8, 210 (1963).

APPENDIX

Calculation of α

The basic equations governing the motion of carriers in an insulator are Poisson's equation and the charge-conservation equation. In equilibrium this last becomes the current-continuity equation. Also the occupation of the levels may be described in terms of a quasi-Fermi level. In the one-dimensional case

$$\partial E/\partial x=(4\pi/\epsilon)\rho \qquad (A1)$$

and

$$J=pe\mu E, \qquad (A2)$$

using the usual symbolism and neglecting diffusion. In the case of an exponential distribution of traps we have at any point

$$p \propto p_t^{\Delta/kT} \equiv p_t^r, \qquad (7)$$

where $r=\Delta/kT$. Neglecting the carriers initially present compared with those injected so that

$$\rho=e(p+p_t)\simeq ep_t$$

we have

$$\frac{dE}{dx}=\frac{4\pi\epsilon}{\epsilon}\beta p^{1/r}=\frac{J}{e\mu}\frac{1}{p^2}\frac{dp}{dx}, \qquad (A3)$$

where β is a constant of proportionality. If it is assumed that the density of carriers at the injecting contact is infinite the solutions for p, p_t, and E are

$$p(x)=p(L)(x/L)^{-r/r+1}, \qquad (A4)$$

$$p_t(x)=p_t(L)(x/L)^{-1/r+1}, \qquad (A5)$$

$$E(x)=E(L)(x/L)^{r/r+1}, \qquad (A6)$$

where L is the specimen thickness.

From Poisson's equation

$$E(L)=\frac{4\pi e}{\epsilon}\int_0^L p_t dx=\frac{4\pi e}{\epsilon}(p_{t\ av})L. \qquad (A7)$$

Also

$$V=-\int_0^L Edx=\frac{r+1}{2r+1}E(L)L=\frac{r+1}{2r+1}\frac{4\pi e}{\epsilon}(p_{t\ av})L^2 \qquad (A8)$$

so that

$$(p_{t\ av})=\alpha V \quad \text{with} \quad \alpha=\frac{2\Delta+kT}{\Delta+kT}\frac{\epsilon}{4\pi eL^2} \qquad (A9)$$